

Parallel, high-resolution carbon and sulfur isotope records of the evolving Paleozoic marine sulfur reservoir

Benjamin C. Gill^{a,*}, Timothy W. Lyons^a, Matt R. Saltzman^b

^a Department of Earth Sciences, University of California-Riverside, Riverside California 92521-0423, USA

^b Department of Geological Sciences, The Ohio State University, Columbus, Ohio 43210, USA

Accepted 15 February 2007

Abstract

Links between the biogeochemical cycles of carbon and sulfur are expressed in the evolving stable isotope composition of the ocean. Carbonate rocks record the inorganic carbon isotope composition of the oceanic reservoir through geological time, along with the sulfate sulfur isotope composition preserved as carbonate-associated sulfate (CAS). An inverse relationship exists between the first-order carbon and sulfur records of the Paleozoic; however, the isotope curves also reveal higher-frequency variations superimposed on the first-order (10^7 – 10^8 yr) trend. Because of links between carbon and sulfur cycling, high-resolution, CAS-based S isotope data have the potential to shed essential light on the mechanisms behind carbon isotope excursions observed in the geologic record.

Results from the Late Cambrian SPICE event at Shingle Pass, Nevada, show parallel positive C (5‰) and S (25‰) isotope excursions, likely recording a large-scale marine organic carbon burial event with sympathetic pyrite burial. Carbon and sulfur records from other events throughout the Paleozoic reveal different and evolving relationships. A Silurian–Devonian boundary section at Strait Creek, West Virginia, reveals a positive C excursion of 6‰ but with an enigmatic, apparently negative S excursion (15‰) antithetic to the C shift. By contrast, a Kinderhookian–Osagean (Early Mississippian) section in the Confusion Range, Utah, shows invariant S isotope ratios across a C isotope excursion of 6‰. The coupling of the high-resolution C–S isotope records may have weakened in the mid-to-late Paleozoic with decreasing sensitivity of the seawater S isotope reservoir to flux changes as the marine sulfate concentrations increased through the Paleozoic. The progressively decreasing isotopic variability of CAS across three positive carbon excursions suggests that the Paleozoic was transitional between a Proterozoic ocean with rapid isotopic variability and thus low sulfate concentration and the comparatively more stable isotopic properties of a relatively more sulfate-rich Mesozoic and Cenozoic ocean. Furthermore, the emergence of the terrestrial ecosystems during the late middle and late Paleozoic yielded new loci of organic burial that also likely played a central role in the decoupling carbon and sulfur isotope records. Organic carbon burial in these sulfate-limited environments occurred in the absence of significant pyrite burial.

© 2007 Elsevier B.V. All rights reserved.

Keywords: Paleozoic; Carbon; Sulfur; Isotope excursions; Paleoceanography; SPICE

1. Introduction

The biogeochemical cycles of carbon and sulfur are intimately linked through biotic and abiotic processes occurring at or near the earth's surface (Berner, 1989).

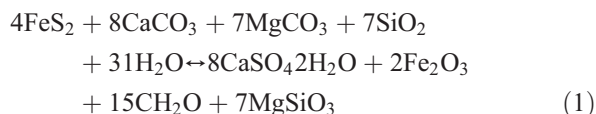
* Corresponding author.

E-mail address: bgill003@ucr.edu (B.C. Gill).

Relationships between the carbon and sulfur cycles are expressed in the evolving stable isotopic properties of the global oceanic reservoir. Perturbations in these cycles, such as enhanced organic matter and pyrite burial or accelerated weathering, can be tracked by the isotope composition of the ocean, with sensitivity dictated by the balance between the relative sizes of the reservoirs and fluxes. For example, when the mass of the seawater reservoir is low as compared to fluxes entering or leaving the ocean, the reservoir is more susceptible to isotopic change (Bartley and Kah, 2004; Kah et al., 2004). Over geologic timescales, the carbon isotope composition of the ocean can be recorded in carbonate minerals found in limestones and dolostones, and the sulfur isotope composition is preserved within evaporative gypsum and anhydrite deposits (Holser and Kaplan, 1966; Claypool et al., 1980; Strauss, 1997; Saltzman et al., 1998; Veizer et al., 1999; Brand, 2004). Additional proxies for the sulfur isotope composition of seawater, such as carbonate-associated sulfate (CAS) and barite,

greatly enhance the resolution and continuity of the sulfur database.

Throughout the Phanerozoic there is a general first-order inverse relationship between the carbon and sulfur isotope records (Fig. 1; Veizer et al., 1980). This relationship has been linked to the mass-balance between the oxidized and reduced reservoirs of the two elements (Veizer et al., 1980; Garrels and Lerman, 1981) through the following equation:



This equation provides the theoretical framework for box models that predict changes in atmospheric $p\text{O}_2$ through the Phanerozoic based on carbon and sulfur isotope trends across this interval (Kump and Garrels, 1986; Berner, 1987, 2001).

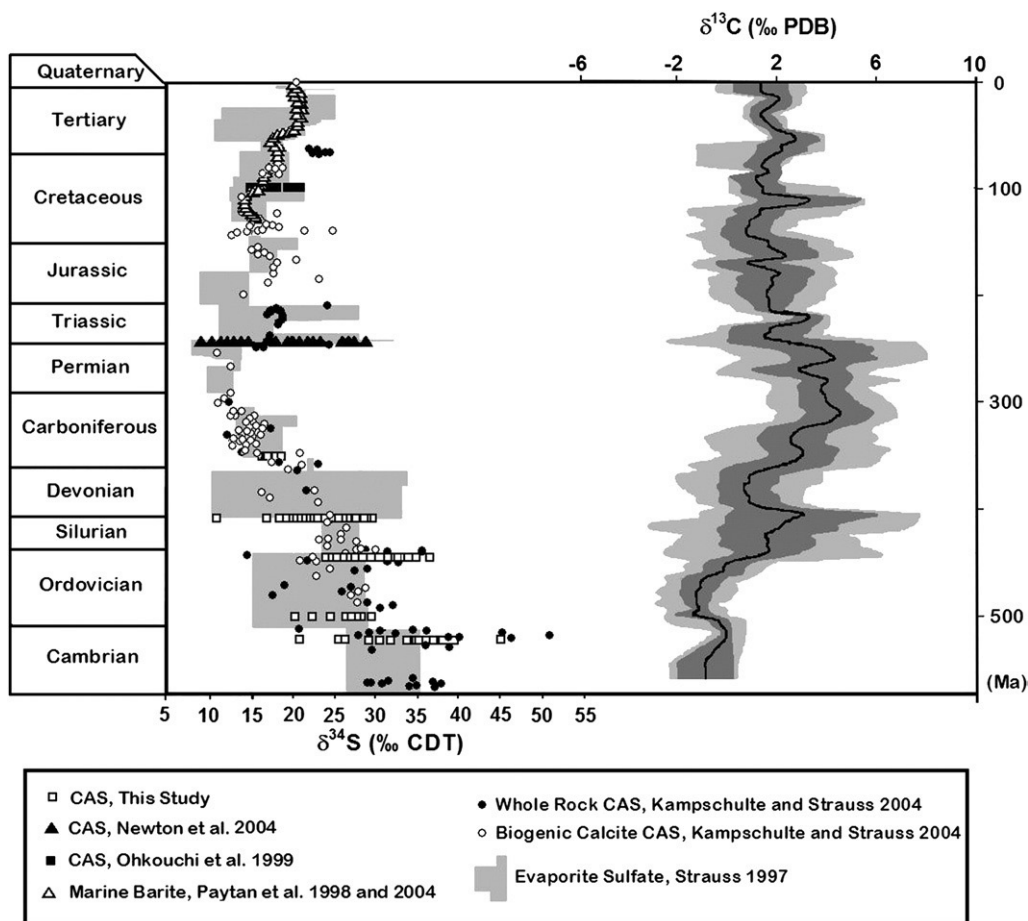


Fig. 1. Carbon and sulfur isotope curves for the Phanerozoic. Modified from Veizer et al. (1999) and Kampschulte and Strauss (2004).

Closer inspection of the isotope curves reveals short-term variability in both the carbon and sulfur isotope data superimposed on the overall first-order trends. Shorter-term variation in the carbon isotope composition of the ocean on the order of 10^6 years has been demonstrated in many earlier studies (e.g., Saltzman et al., 1998; Kump et al., 1999; Saltzman et al., 2000; Saltzman, 2002a, 2002b). However, only recently has variation on the same time scales been documented for sulfur isotopes (Paytan et al., 1998; Ohkouchi et al., 1999; Paytan et al., 2004; Newton et al., 2004; Riccardi et al., 2006), including patterns seen in detailed data sets for the Proterozoic (Hurtgen et al., 2002; Kah et al., 2004; Gellatly and Lyons, 2005; Fike et al., 2006).

This study is part of a continuing investigation examining parallel carbon and sulfur isotope records across previously documented, 10^6 -year perturbations in the carbon cycle expressed as positive carbon isotope excursions during the Paleozoic. Our preliminary results show that sulfur data do track changes in the carbon cycle but with patterns of isotopic variability that change through time. These different responses in the sulfur isotope record shed light on the mechanisms behind each carbon isotope excursion. More specifically, CAS data appear to decrease in variability across progressively younger carbon isotope excursions in the Paleozoic, suggesting an increase in the oceanic sulfur reservoir spanning the Paleozoic and/or fundamental shifts in the locus of organic carbon burial. Such trends have important implications for the evolution of oxygen in the atmosphere: the redox history of the earth's oceans; and evolution in the earth's biosphere, including the increasing role of terrestrial carbon burial.

1.1. Biogeochemistry of sulfur cycle and its links to the carbon cycle

The major input of sulfur to the ocean reservoir is sulfate from runoff derived from the weathering of sulfides and sulfate minerals on the continents. The isotopic composition of this runoff reflects the combined isotopic properties of the weathered constituents, with an average modern value lying between 0–10‰ (Holser et al., 1988) relative to the +20‰ sulfur isotope composition of present-day seawater. Other important inputs to the ocean reservoir include magmatic sulfur derived either from mid-ocean ridges or volcanism on land, which also have an isotope composition of 0–10‰. Since these higher temperature inputs are thought to be quantitatively minor as compared to continental runoff during the Phanerozoic, they have largely been ignored in numerical models applied to the ocean reser-

voir during this time period (Kump, 1989; Petsch and Berner, 1998; Berner, 2001; compare Carpenter and Lohmann, 1997; Carpenter and Lohmann, 1999).

Removal of sulfur from the ocean occurs through two major pathways: precipitation of sulfate minerals during evaporite deposition and the burial of pyrite. Precipitation of sulfate minerals during evaporation of seawater has only a small associated fractionation of 0–3‰, and therefore evaporite deposition does not impart a substantial isotope effect on the ocean reservoir (Ault and Kulp, 1959; Thode et al., 1961, Holser and Kaplan, 1966; Raab and Spiro, 1991).

Pyrite burial is the major sink of sulfur in the modern ocean and occurs in anoxic sediments in association with bacterial sulfate reduction (BSR). Pyrite forms through reactions between the hydrogen sulfide formed during BSR and detrital iron-bearing minerals (Berner, 1970; Berner, 1984). BSR imparts a strong fractionation between the sulfate and pyrite reservoirs by preferentially utilizing the lighter isotope, ^{32}S , leaving the residual sulfate reservoir enriched in the heavier ^{34}S . The H_2S deriving from BSR can be up to 40–45‰ depleted in ^{34}S relative to the parent sulfate (Harrison and Thode, 1957; Kemp and Thode, 1968; Habicht and Canfield, 1997; Canfield, 2001; Detmers et al., 2001). However, fractionations of up to 70‰ between sulfate and pyrite in modern and ancient environments have been explained by redox recycling and associated disproportionation reactions (Canfield and Thamdrup, 1994; Habicht and Canfield, 1996, 1997, 2001; compare Brunner and Bernasconi, 2005).

Despite the preferential reduction of ^{32}S , bacteriogenic pyrite can display broad isotope ranges, including very positive and negative $\delta^{34}\text{S}$ values, which track the sulfate reservoir properties, the redox conditions, the pathways of oxidation and disproportionation, and the initial kinetic controls (e.g., rates of BSR) (Detmers et al., 2001; Canfield, 2001; Habicht and Canfield, 2001).

The sulfur and carbon cycles are related through two key processes. Continental weathering links these cycles since it is not only a major source of sulfur to the ocean reservoir, but also one for carbon through the weathering of carbonates and organic matter. The coupled burial of pyrite and organic matter in marine sediments also links the sulfur and carbon cycles. There is a positive correlation between organic matter and pyrite burial in modern and ancient “normal” marine sediments, which accumulate beneath oxic bottom waters (Berner and Raiswell, 1983). This relationship seems counterintuitive because organic matter is oxidized during bacterial sulfate reduction. However, in normal marine systems organic carbon is often the limiting species for BSR and

thus diagenetic pyrite formation. Therefore, increased organic matter burial can enhance sulfate reduction and pyrite burial, although iron availability also plays a role, even under oxic depositional conditions (Berner and Raiswell, 1983; Canfield et al., 1992).

The relationship between carbon and sulfur burial can be fundamentally different in euxinic and terrestrial environments, where Fe and sulfate limitations, respectively, often prevail. In terrestrial systems sulfate is often limiting, leading to low rates of BSR and thus pyrite burial. In euxinic environments (those containing hydrogen sulfide in the water column), iron is often the limiting reactant in pyrite formation. The relative extent and magnitude of carbon burial in these different surficial environments (terrestrial, normal marine, and euxinic) can impact the carbon and sulfur isotope chemistry of the ocean over geologic time.

Variability in the sulfur isotope composition of oceanic sulfate can be used to track the balance between evaporite deposition, pyrite burial, and pyrite and evaporite weathering (Berner and Raiswell, 1983). Very positive values of $\delta^{34}\text{S}$ in the ocean reservoir reflect enhanced burial of pyrite, whereas $\delta^{34}\text{S}$ values close to the range of riverine input of 0–10‰ reflect pyrite weathering with or without evaporite deposition. Because the sulfur isotope composition of seawater is a fingerprint of pyrite burial and weathering, comparisons of coeval carbon and sulfur isotope records can illuminate the mechanisms behind carbon isotope excursions present throughout geologic time.

1.2. Isotope proxies for carbon and sulfur

The inorganic carbon isotope ($\delta^{13}\text{C}_{\text{carb}}$) composition of the ocean can be preserved in marine carbonates in the geologic record (Saltzman et al., 1998; Veizer et al., 1999; Brand, 2004). Fortunately, carbonate rocks are abundant, allowing for relatively continuous and high-resolution data for much of the Phanerozoic. Biogenic calcite from pristine brachiopods is thought to be the most reliable recorder of seawater stable isotope compositions (carbon, oxygen, strontium, and sulfur) (Popp et al., 1986; Veizer et al., 1986; Carpenter and Lohmann, 1995; Veizer et al., 1999; Mii et al., 1999; Kampschulte et al., 2001; Brand, 2004; Kampschulte and Strauss, 2004; compare Parkinson et al., 2005), but distributions of brachiopods are rarely continuous enough to produce complete, high-resolution, meter-scale, chemostratigraphic profiles over broad stratigraphic thicknesses. Given these gaps, micritic constituents are an attractive alternative (Kaufman et al., 1991; Saltzman et al., 1998; Kump et al., 1999; Saltzman et al., 2000), particularly

during the Precambrian when skeletal remains are absent. Secondary alteration is always a concern, but small-scale heterogeneities may be averaged in whole-rock samples during early, low temperature diagenesis (Saltzman et al., 1998). Also, the carbon isotope properties of carbonates are buffered to rock values during diagenesis because of the low concentrations of carbon in diagenetic fluids as compared to the volume of rock (Banner and Hanson, 1990; Frank and Lohmann, 1996; Carpenter and Lohmann, 1997).

The sulfur isotope record of ancient seawater is less established. Past work has emphasized gypsum and anhydrite (Holser and Kaplan, 1966; Claypool et al., 1980; Strauss, 1997; Kah et al., 2001); however, evaporite deposition was episodic and highly localized through geologic time, and gypsum and anhydrite have a relative poor preservation potential. Evaporites are also difficult to date due to a lack of biostratigraphically useful fossils and material suitable for isotopic dating and must rely on strata located adjacent to these deposits. These factors have contributed to a fragmented, lower resolution sulfur isotope record for the Phanerozoic and particularly the Precambrian.

1.3. Carbonate-associated sulfate as a proxy for seawater sulfate

Proxies for the sulfur isotope composition of seawater other than gypsum and anhydrite have proven value for refined isotopic characterizations of the ancient ocean. Methodologies now widely used emphasize marine barites, trace sulfate in phosphates, and trace sulfate in carbonates (Cecile et al., 1983; Burdett et al., 1989; Paytan et al., 1998; Hurtgen et al., 2002; Paytan et al., 2004; Shields et al., 2004; Gellatly and Lyons, 2005; Goldberg et al., 2005). Each approach has its strengths and weaknesses, but none has the potential to provide the spatial and temporal coverage afforded by CAS.

Carbonate-associated sulfate occurs as a trace constituent within carbonate minerals, substituting for the CO_3^{2-} group (Takano, 1985; Pingitore et al., 1995). Modern biogenic carbonates typically contain CAS concentrations of 1000–10,000 ppm, and ancient limestones and dolomites generally show concentrations ranging from 0 to 1000 ppm (Staudt and Schoonen, 1995; Kampschulte et al., 2001; Kampschulte and Strauss, 2004; Lyons et al., 2004a). The sulfur isotope composition of CAS ($\delta^{34}\text{S}_{\text{CAS}}$) in modern biogenic carbonates and bulk micrite typically matches that of contemporaneous seawater within 1‰ (Burdett et al., 1989; Strauss, 1999; Kampschulte et al., 2001;

Kampschulte and Strauss, 2004; Lyons et al., 2004a), and $\delta^{34}\text{S}_{\text{CAS}}$ records are in good agreement with coeval evaporite deposits spanning the geologic record (Burdett et al., 1989; Strauss, 1999; Kampschulte et al., 2001; Kah et al., 2004; Kampschulte and Strauss, 2004).

Although CAS was first analyzed for its sulfur isotope composition by Ueda et al. (1987), it was not until the pioneering study by Burdett et al. (1989) that CAS (in Neogene calcareous microfossils) was used to generate a seawater sulfur isotope curve. To date, the CAS proxy has been applied most extensively in studies of the Precambrian (Ueda et al., 1991; Hurtgen et al., 2002; Kah et al., 2004; Hurtgen et al., 2005; Gellatly and Lyons, 2005; Goldberg et al., 2005; Fike et al., 2006), yielding high-resolution sulfur isotope curves across intervals generally lacking gypsum and anhydrite. Only a few high-resolution CAS studies have focused on Phanerozoic strata. Importantly, Kampschulte et al. (2001) and Kampschulte and Strauss (2004) used CAS to validate and refine the Phanerozoic marine sulfur curve of Claypool et al. (1980) by filling in gaps within the evaporite record. High-resolution records are available for key intervals in the Phanerozoic including the Permian–Triassic and Cenomanian–Turonian boundaries (Ohkouchi et al., 1999; Newton et al., 2004; Riccardi et al., 2006).

2. Locations and samples

To investigate the behavior of marine sulfur isotope record and possible linkages between the carbon and sulfur isotope systems we have looked at time intervals that contain three well-studied, globally expressed carbon isotope excursions. For comparison, our study also includes an interval lacking pronounced carbon isotope variability. Our sampling emphasizes previously described Paleozoic sections (Silberling et al., 1997; Saltzman et al., 1998, 2000; Overstreet et al., 2003). All of the sections, with the exception of Shingle Pass location, lack previous carbon isotope analysis. No previous sulfur isotope data were available. In most instances, the $\delta^{13}\text{C}_{\text{carb}}$ and $\delta^{34}\text{S}_{\text{CAS}}$ data were generated from the same sample.

2.1. Late Cambrian

The Upper Cambrian section exposed at Shingle Pass, Eagan Range, Nevada, spans more than 300 m and contains, in ascending order, the Emigrant Springs Limestone, Johns Walsh Limestone, Corset Shale, and Whipple Cave Formation. The Johns Wash Limestone consists of heterogeneous carbonate facies that include

peloidal grainstones, ooid grainstones, wackestones, flat-pebble conglomerates, and thrombolitic boundstones. This unit lies entirely within the Steptoean Stage (see Saltzman et al., 1998 for a detailed description of the sedimentology). Previous work on this section documented the existence of the globally correlated Steptoean Positive Carbon Isotope Excursion, or SPICE event, which is bounded by two major trilobite extinctions (Glumac and Walker, 1998; Saltzman et al., 1998; Saltzman et al., 2000; Cowan et al., 2005).

2.2. Early Ordovician

Samples were collected from the Lower Ordovician Gasconade Formation located outside Jerome, Missouri. Overstreet et al. (2003) described this section as part of a more general investigation of cyclic carbonate facies in the Lower Ordovician. However, no previously published work explored the carbon isotope stratigraphy. The Gasconade Formation at this location consists of variable but cyclic dolomitized carbonate facies, including peloidal grainstones, ooid grainstones, micrite mudstones, interbedded chert nodules, chert beds, and stromatolites. The Gasconade Formation was selected because the Early Ordovician Ibexian Stage is devoid of any known large carbon isotope excursions (Buggisch et al., 2003). A lack of perturbation in the carbon cycle, as expressed in relative carbon isotope stability, allowed us to evaluate background CAS behavior in the absence of pronounced carbon isotope variability. As such, dramatic fluctuations in $\delta^{34}\text{S}_{\text{CAS}}$ could reflect diagenesis or some primary control unrelated to carbon isotope behavior.

2.3. Silurian–Devonian boundary

The section located at Strait Creek, West Virginia, exposes rocks of the Helderberg Group and consists, in ascending order, of the Upper Keyser, New Creek, and Corriganville limestones, which span the Silurian–Devonian boundary. The Upper Keyser Limestone is 35 m thick at this location and consists mainly of wackestone and packstone. The Upper Keyser grades into the overlying crinoidal packstone to grainstone of the New Creek Limestone, which spans the middle 11 m of the section. The Corriganville Limestone is finer-grained and comprises the upper 5 m of the measured section. The Helderberg Group exposed at nearby Smoke Hole, West Virginia, contains a positive inorganic carbon excursion of $\sim 5\%$, which, like the SPICE event, has been globally correlated (Hladikova et al., 1997; Saltzman, 2002b; Buggisch and Mann, 2004).

2.4. Early Mississippian

The Lower Mississippian was sampled in the Confusion Range, Utah. This approximately 80 meter section spans the Kinderhookian–Osagean stage boundary. The stratigraphy of this section, which consists entirely of the Joana Limestone, was documented in detail by Silberling et al. (1997). The lithology of the Joana at this location is dominated by wackestones and crinoidal grainstones and packstones (Silberling et al., 1997). The Joana Limestone is overlain by the shaly and dolomitic Needles Siltstone. The Kinderhookian–Osagean stage boundary has a well-documented carbon excursion, which correlates globally among carbonates in Belgium, the Ural Mountains, midcontinent North America, and other localities in Nevada (Bruckschen and Veizer, 1997; Bruckschen et al., 1999; Mii et al., 1999; Saltzman, 2002a; Saltzman et al., 2004).

3. Methods

Following collection of 25 to 100 g carbonate samples, the materials were cut on a water-cooled saw to remove weathered surfaces and secondary veins. A portion of the cut rock was set aside for analysis of carbon isotopes for all samples other than those from the Upper Cambrian Shingle Pass section. We microdrilled

freshly cut outcrop material for carbon isotope analysis using a dental drill and emphasizing the finest-grained, most micritic portions in an effort to avoid secondary phases such as course spar and late diagenetic veins; the validity of this approach is documented in Kaufman et al. (1991), Saltzman et al. (1998), and Kump et al. (1999).

The drilled powders were roasted at 380 °C for one hour to remove volatile phases prior to analysis. The carbonate powders were then analyzed at the University of Michigan stable isotope lab where they were reacted with 100% phosphoric acid at 75 °C in an online carbonate preparation device (Carbo-Kiel single-sample acid bath) connected to a Finnigan Mat 251 isotope ratio mass spectrometer. The drilled powders from the Gasconade Formation were analyzed at the University of Missouri stable isotope lab using a Finnigan-Mat Delta Plus gas source mass spectrometer with online Kiel III device for automated C and O isotope analysis. In all cases, carbon isotope compositions are expressed in standard delta notation as per mil (‰) deviations from Vienna Pee Dee Belemnite (V-PDB), with an analytical error of 0.04‰ for the Straight Creek and Confusion Range samples and 0.02‰ for the Gasconade Formation.

We crushed the remaining samples in a shatter box to fine powders suitable for CAS analysis. Approximately 25 to 100 g (~60 g on average) of the fine powder from each sample were then treated with two deionized water

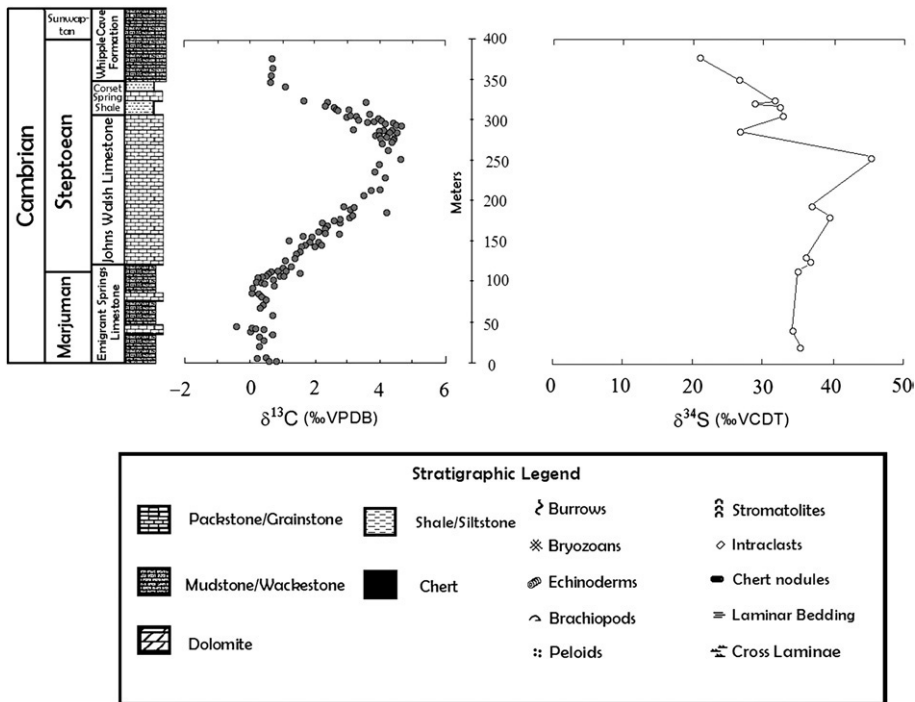


Fig. 2. δ¹³C and δ³⁴S curves CAS sulfur and carbonate carbon, Shingle Pass Section, Nevada.

rinses lasting 24 hours each. These water rinses removed any soluble sulfates that may have been present in the rocks. After each rinse, the overlying water was carefully decanted. We then treated the samples in a 4% hypochlorite solution for 48 hours to remove any metastable sulfides and organically bound sulfur. Two

more deionized water rinses followed before the samples were dissolved using 4 N HCl. The resulting sample was centrifuged and then vacuum filtered (45 μm) to remove the insoluble portion of the sample.

Approximately 100 mL of a saturated BaCl_2 solution (250 g/L) was added to the remaining solution to

Table 1
Stable isotope data for CAS sulfur and carbonate carbon, Shingle Pass, Nevada

Interval (m)	$\delta^{34}\text{S}$ (‰, VCDT)	$\delta^{13}\text{C}$ (‰, VPDB)	Interval (m)	$\delta^{34}\text{S}$ (‰, VCDT)	$\delta^{13}\text{C}$ (‰, VPDB)	Interval (m)	$\delta^{34}\text{S}$ (‰, VCDT)	$\delta^{13}\text{C}$ (‰, VPDB)
1.4		0.82	119		1.28	282.8		3.99
2.8		0.57	123.2		1.11	285.6	26.7	4.3
4.2		0.49	126	36.9	1.13	286.3		4.52
5.6		0.24	130.2	36.5	1.41	287		3.95
19.6	35.6	0.32	134.4		1.42	287.7		4.34
28		0.44	137.2		1.55	288.4		4.1
30.8		0.3	138.6		1.52	289.8		3.17
35		0.66	142.8		1.59	294		
39.2		0.02	144.2		1.98	295.1		4.65
40.6	34.5	0.45	145.6		1.71	295.4		4.54
42		0.18	147		2.18	296.2		4.42
43.4		0.1	148.4		2.12	296.8		4.16
44.8		-0.41	149.8		1.86	298.2		3.61
58.8		0.69	151.2		1.19	299		3.85
68.6		0.34	155.1		1.92	299.6		4.09
70		0.42	155.4		1.93	301		3.97
78.4		0.47	156.8		1.64	302.4		3.33
79.8		0.5	159.6		2.76	304.5	33.3	2.96
84		0.37	161		2.33	304.9		3.27
86.1		0.28	162.4		2.15	306.6		3.11
86.8		0.08	163.8		2.33	308		3.7
93.8		0.11	166.6		2.33	313.6		3.06
95.2		0.77	169.4		2.38	315		2.64
98		0.31	172.2		2.25	316.4	32.6	2.6
98.4		0.47	173.6		2.79	320.6	29.1	2.37
99.4		0.27	176.4		2.59	322.3		3.59
100.5		0.41	177.8		2.8	322.98	32.0	
100.8		0.53	180.6	39.7	3.13	323		2.4
101		0.2	183.4		3.18	324.8		1.66
103		0.73	186.2		4.19	341.6		1.11
103.7		0.46	189		3.11	348.6		0.68
104.2		0.26	191.8		3.23	350	26.8	
104.7		0.49	193.2	37.3	2.91	355.6		0.67
105		0.25	208.6		3.5	364.7		0.71
105.1		0.53	212.8		3.73	376.6	21.2	0.72
105.4		0.37	214.2		4.02			
106		0.51	229.6		4.17			
106.4		0.42	238		3.84			
107		0.98	245		4			
107.4		0.97	252	45.7	4.65			
107.5		1.05	263.2		4.23			
109		0.61	273		4.04			
110		1.57	274.4		4.35			
112.9		0.67	277.2		4.43			
113.4	35.1	0.86	278.9		4.02			
114.8		0.95	279		4.2			
116.2		1.13	280		4.19			
117.6		1.05	281.4		3.86			

precipitate sulfate as BaSO_4 . We let the samples sit for at least three days to ensure complete precipitation. The BaSO_4 was separated from the remaining solution via filtration and allowed dry. The BaSO_4 powders were then homogenized and loaded into silver capsules with excess V_2O_5 and analyzed for their $^{34}\text{S}/^{32}\text{S}$ isotope ratios at the University of Indiana-Bloomington using a Finnigan MAT 252 gas source mass spectrometer fitted with an elemental analyzer for online sample combustion and analysis. All sulfur isotope compositions are expressed in standard delta notation as per mil (‰) deviations from Vienna Canyon Diablo Troilite (V-CDT) with analytical errors of less than 0.2‰.

4. Results

4.1. Late Cambrian SPICE event

A $\delta^{13}\text{C}_{\text{carb}}$ excursion was documented previously at Shingle Pass by Saltzman et al. (1998) and is reproduced here for comparison to our sulfur isotope data (Fig. 2, Table 1). Carbon isotope values of approximately 0‰ in the Emigrant Springs Limestone gradually climb from 0‰ at the base of the John Walsh Limestone to values in excess of +5‰ over 250 m of section. The data rapidly decrease over the upper 100 m of the section—quickly declining in the Corset Springs Shale and leveling off at values around 0‰ in the Whipple Cave Formation. CAS

records a positive sulfur isotope excursion in excess of +25‰ over the measured section. Values in the Emigrant Springs Limestone start at approximately +35‰ and gradually peak at +45‰ at the top of the John Walsh Limestone. The $\delta^{34}\text{S}_{\text{CAS}}$ data drop dramatically from +45‰ to +26‰ in the Corset Shale but then rise to values around +30–33‰ in the Whipple Cave Formation. $\delta^{34}\text{S}_{\text{CAS}}$ in the Whipple Cave Formation then declines to +21‰ over the remainder of the measured section. Carbon and sulfur isotopes vary sympathetically over the full extent of the analyzed section, reaching their maximum and minimum values at the same stratigraphic levels.

4.2. Early Ordovician

The $\delta^{13}\text{C}_{\text{carb}}$ and $\delta^{34}\text{S}_{\text{CAS}}$ records of the Early Ordovician Jerome Section are essentially homogenous (Fig. 3, Table 2). Carbon isotope values range from -1.5 to -2‰ over the entire length of the measured section. $\delta^{34}\text{S}_{\text{CAS}}$ shows some minor variability over most of the section with a maximum variation of 9‰. This shift occurs near the base of the section with a value of +24‰ that drops to +19‰, then increases to +28‰, and finally drops back to values around +24‰. There is an overall increase in the sulfur isotope values from +24‰ to around +26‰ over the rest of the measured section.

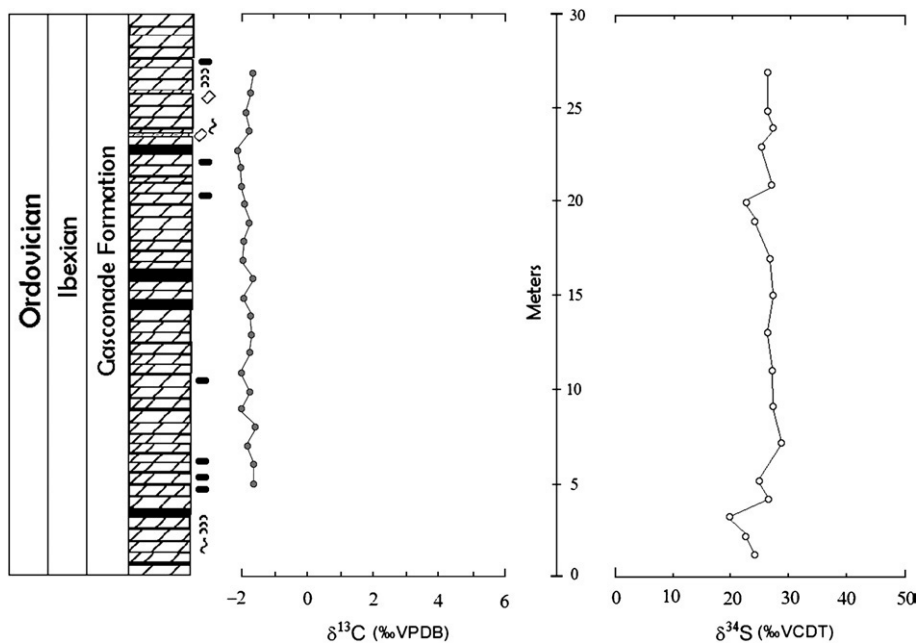


Fig. 3. $\delta^{13}\text{C}$ and $\delta^{34}\text{S}$ curves for CAS sulfur and carbonate carbon, Gasconade Formation, Jerome, Missouri. Symbol legend is provided with Fig. 2.

Table 2
Stable isotope data for CAS sulfur and carbonate carbon, Jerome, Missouri

Interval (m)	$\delta^{34}\text{S}$ (‰, VCDT)	$\delta^{13}\text{C}$ (‰, VPDB)
1	24.0	
2	22.5	
3	19.7	
4	26.3	
5	24.8	-1.66
6		-1.67
7	28.6	-1.85
8		-1.60
9	27.0	-2.06
10		-1.79
11	27.0	-2.02
12		-1.77
13	26.2	-1.71
14		-1.74
15	27.1	-1.95
16		-1.69
17	26.7	-2.00
18		-1.97
19	24.0	-1.78
20	22.5	-1.90
21	26.8	-2.03
22		-2.04
23	25.1	-2.13
24	27.1	-1.77
25	26.2	-1.88
26		-1.76
27	26.3	-1.70

4.3. Silurian–Devonian boundary event

The carbon isotope record at Strait Creek is similar in magnitude to those described for other sections of the same age in North America and Europe by Saltzman (2002b) and Buggisch and Mann (2004) (Fig. 4, Table 3). The excursion occurs low in the section in the Upper

Keyser, spanning from the 10 and 30 meter marks in the measured interval. $\delta^{13}\text{C}_{\text{carb}}$ quickly peaks at values that vary between +4 and +6‰. The carbon isotopes then fall to +2‰ at the Upper Keyser–New Creek contact and then rise again to +3.7‰ in the New Creek before decreasing gradually to +1.5‰ in the Corriganville Limestone. The CAS data show considerable variability over the lower half of the section, with values ranging from +10.9 to +26.9‰. Despite these fluctuations, the $\delta^{34}\text{S}_{\text{CAS}}$ values for the lower half of the section are distinctly less than those for the upper half. Five meters from the top of the Upper Keyser, $\delta^{34}\text{S}_{\text{CAS}}$ becomes considerably less variable and jumps from +20‰ to +30‰ in the New Creek Limestone. At the top of the measured section, the $\delta^{34}\text{S}_{\text{CAS}}$ values fall to approximately +25‰ in the Corriganville Limestone. The relationship between the carbon and sulfur isotopes is less clearly defined in the Strait Creek section although an antithetic relationship is present; the lowest sulfur values correspond with the peak of the carbon isotope excursion and increase over the falling limb of the carbon isotope excursion.

4.4. Early Mississippian event

The magnitude of the carbon isotope excursion recorded at the Confusion Range in Utah is consistent with those measured in other sections of the same age in Nevada and Europe (Fig. 5, Table 4; Bruckschen and Veizer, 1997; Bruckschen et al., 1999; Saltzman, 2002a, 2004). $\delta^{13}\text{C}_{\text{carb}}$ values at the base of the section in the Joana Limestone start between 0 and +1‰ and climb to approximately +2.5‰, where they plateau. Forty meters into the measured section the values start to increase rapidly and by 51 m they reach +6.1‰. $\delta^{13}\text{C}_{\text{carb}}$ then decreases to values between 0 and +1‰ over the upper

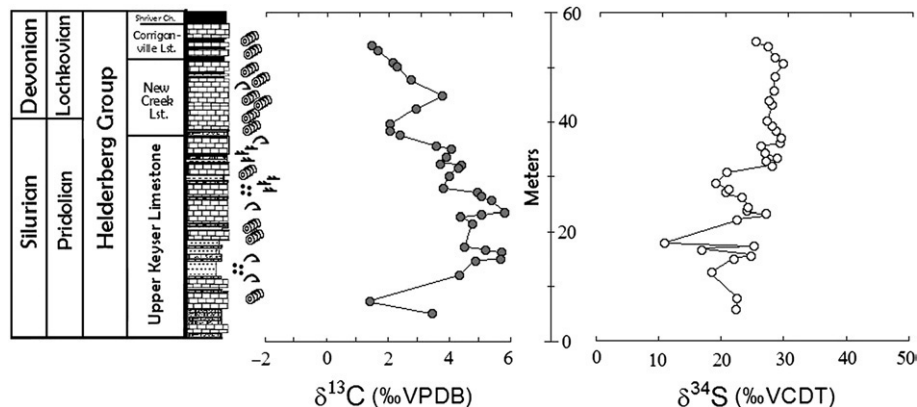


Fig. 4. $\delta^{13}\text{C}$ and $\delta^{34}\text{S}$ curves for CAS sulfur and carbonate carbon, Helderberg Group, Strait Creek, West Virginia. Symbol legend is provided with Fig. 2.

30 m of the Joana Limestone, with an anomalous value of +2‰ in the uppermost sample. $\delta^{34}\text{S}_{\text{CAS}}$ values, unlike the carbon isotope data, show little variation, with maximum variation over the entire section of about 3‰ spanning from +16.8 and +19.7‰.

5. Discussion

The biogeochemical cycles of sulfur and carbon are coupled through a network of input and output fluxes that are linked to the ambient environmental conditions. Because the sulfur cycle is intimately linked to the carbon cycle through organic matter and pyrite burial and continental weathering, examining the two isotope

records in parallel across each of the events in our investigation can shed light on the potential mechanisms driving both isotope systems.

5.1. SPICE event

A relationship between the sulfur and carbon isotope systems is apparent in the Late Cambrian Shingle Pass section with its parallel, positive excursions in the $\delta^{34}\text{S}$ and $\delta^{13}\text{C}$ records. Previously, the carbon isotope trend was attributed to enhanced marine primary productivity and organic matter burial, which preferentially removal of ^{12}C from the oceanic reservoir (Saltzman et al., 1998, 2000). In light of this previous interpretation we interpret the positive $\delta^{34}\text{S}_{\text{CAS}}$ trend as reflecting enhanced pyrite burial, stimulated by increased organic matter burial during the SPICE event. The increased pyrite burial preferentially removed ^{32}S from the oceanic reservoir, resulting in the parallel, positive CAS behavior.

An interesting observation, although our data are limited, is the possible establishment of a new baseline in the $\delta^{34}\text{S}_{\text{CAS}}$ data after the event, which is shifted by 10–15‰ relative to pre-excursion values (30–35‰). The data of Kampschulte and Strauss (2004), although at coarser resolution, are consistent with a post-SPICE $\delta^{34}\text{S}_{\text{CAS}}$ drop, but the bulk of their CAS data from immediately after the SPICE fall around +30‰. Absent finer sample resolution for their data, further speculation is not warranted. Our ongoing exploration of the post-SPICE interval is further exploring this relationship further.

5.2. Early Ordovician record

The monotonous carbon and sulfur isotope records of the Early Ordovician Gasconade Formation suggest that short-term $\delta^{34}\text{S}_{\text{CAS}}$ variability in the Early Paleozoic is indeed driven by perturbations in the carbon cycle. It should be mentioned, however, that these rocks have been heavily dolomitized. Carbonate lithologies and vugs in the Gasconade Formation point to the possibility of primary or very early replacement dolomite formation within a sabkha environment, but coarse secondary dolomites that are likely the product late/burial dolomitization are also pervasive. Despite this, carbon isotopes from this section match values derived from brachiopod calcite for this same time period from a variety of North American basins (Qing and Veizer, 1994; Veizer et al., 1999). This consistency is to be expected, as carbon isotopes are commonly buffered from isotopic change due to the low amount of carbon present in secondary fluids (Banner and Hanson, 1990; Saltzman et al., 1998;

Table 3
Stable isotope data for CAS sulfur and carbonate carbon, Strait Creek, West Virginia

Interval (m)	$\delta^{34}\text{S}$ (‰, VCDT)	$\delta^{13}\text{C}$ (‰, VPDB)
5	22.3	3.40
7	22.4	1.40
12	18.2	4.26
14.5	21.9	4.81
15	24.7	5.62
16	16.8	5.67
16.5	25.2	5.09
17	11.0	4.44
21.5	22.5	4.73
22.5	27.0	4.32
23	23.9	5.00
23.5	24.0	5.75
25.5	23.3	5.29
26.5	20.5	4.99
27	21.2	4.92
28	19.0	3.75
30	20.8	3.95
31.5	28.0	4.23
32	27.2	4.33
32.5	29.0	3.66
33.5	26.9	3.86
35	26.1	4.03
35.5	29.4	3.54
36.5	29.4	
37.5	28.7	2.35
38.5	28.1	2.06
39.5	27.0	2.06
42.5	28.0	2.90
43	27.3	
45	28.5	3.76
47.5	28.5	2.73
50	29.8	2.27
51	28.5	2.14
53	27.4	1.66
54	25.7	1.46

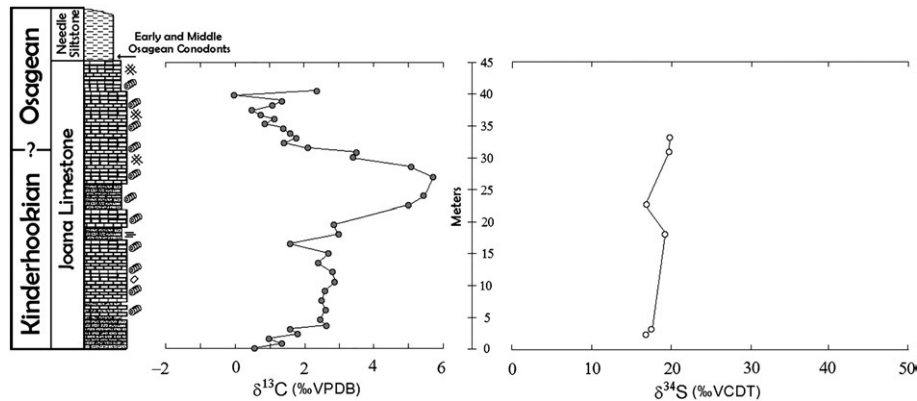


Fig. 5. $\delta^{13}\text{C}$ and $\delta^{34}\text{S}$ curves for CAS sulfur and carbonate carbon, Joana Limestone, Confusion Range, Utah. Symbol legend is provided with Fig. 2.

Veizer et al., 1999; Brand, 2004). It is possible that the sulfur isotopes in the CAS have been altered or homogenized by later dolomitizing fluids. However, wholesale resetting of primary $\delta^{34}\text{S}_{\text{CAS}}$ seems unlikely: there is a strong match between our $\delta^{34}\text{S}_{\text{CAS}}$ values and those from Kampschulte and Strauss (2004) and the evaporite data for the Early Ordovician compiled in Strauss (1997). Also, despite pervasive meteoric diagenesis in the Key Largo Limestone of the Florida Keys, the isotopic composition of CAS is buffered against isotopic change (Lyons et al., 2004b). Such buffering may also be true for dolomitizing fluids with low concentrations of sulfate or with the $\delta^{34}\text{S}$ properties of the overlying seawater under conditions of very early dolomitization. Our continuing work in other sections outside and within carbon excursions will rigorously test the integrity and local versus global relevance of the data presented here.

5.3. Silurian–Devonian boundary event

Relationships expressed in the isotope systematics of the Silurian–Devonian event are less straightforward than those of the SPICE event. The CAS data do, however, attain more-depleted $\delta^{34}\text{S}$ values during the peak of the positive carbon excursion; $\delta^{34}\text{S}_{\text{CAS}}$ values then become more positive and uniform after the carbon excursion. This response is opposite that of the SPICE event. One possible mechanism for the observed carbon isotope record is the weathering hypothesis put forth by Kump et al. (1999) for the Late Ordovician positive carbon excursion. By their scenario, a lowering of sea-level caused by southern hemisphere glaciations exposed shallow-water carbonate platforms to weathering. This exposure resulted in an increased flux of weathered carbonate carbon, resulting in the positive carbon excursion.

An increased input of more ^{13}C -enriched carbon during a eustatic drop in sea-level could explain the carbon excursion also seen in the Silurian–Devonian boundary event. The mechanism for the corresponding negative sulfur isotope shift would be enhanced pyrite weathering from the exposed continental shelves, which would increase the flux of $\delta^{34}\text{S}$ -depleted sulfur to the ocean and result in antithetic behavior between $\delta^{13}\text{C}_{\text{carb}}$ and $\delta^{34}\text{S}_{\text{CAS}}$. No evidence exists for glaciation across the Silurian–Devonian boundary. Nevertheless, Saltzman (2002b) cited stratigraphic data, coarsening lithologies, and unconformities from North America basins in Oklahoma and Nevada as evidence for a drop in sea-level across the boundary. Buggisch and Mann (2004) noted that the Silurian–Devonian boundary is marked by transgressive sequences in Europe and Australia, which is inconsistent with the suggested global drop in sea-level.

A second hypothesis for the carbon isotope record across the Silurian–Devonian boundary is an organic matter burial event (Saltzman, 2002b; Buggisch and Mann, 2004). However, the $\delta^{34}\text{S}_{\text{CAS}}$ record does not indicate parallel pyrite burial, in contrast to the SPICE event. Buggisch and Mann (2004) argued for a combination of enhanced carbonate weathering coupled with enhanced organic matter burial stimulated by increased nutrient flux from weathering during the Caledonian/Acadian orogeny. To be consistent with our isotopic record, any enhanced pyrite burial, which may have resulted from the increased organic matter burial, would have been minor compared to the enhanced flux of $\delta^{34}\text{S}$ -depleted sulfur to the ocean. $\delta^{34}\text{S}$ -depleted sulfate may have been supplied from accelerated weathering during the Caledonian/Acadian orogeny and/or from exposed, contemporaneous shelf deposits. Additional parallel isotope records for this time period extending further above and below the excursion, in combination with

Table 4
Stable isotope data for CAS sulfur and carbonate carbon, Confusion Range, Utah

Interval (m)	$\delta^{34}\text{S}$ (‰, VCDT)	$\delta^{13}\text{C}$ (‰, VPDB)
0		0.56
1.5		1.36
3		0.97
4.5	16.9	1.82
6	17.5	1.59
7.5		2.64
9		2.45
12		2.62
15		2.51
18		2.60
21		2.87
24		2.82
27		2.41
30		2.71
33		1.59
36	19.2	3.00
39		2.86
45	16.8	5.01
48		5.46
51		6.12
54		5.67
57		5.09
60		3.40
61.5	19.6	3.52
63		2.10
64.5		1.39
66	19.7	1.77
67.5		1.60
69		1.39
70.5		0.86
72		1.14
73.5		0.74
75		0.48
76.5		1.08
78		1.36
79.5		-0.02
81		2.36

numerical modeling, will better define the exact relationship between the carbon and sulfur sources and sinks.

5.4. Synthesis of Paleozoic carbon and sulfur isotope records

The combined high-resolution $\delta^{34}\text{S}_{\text{CAS}}$ and $\delta^{13}\text{C}_{\text{carb}}$ data reveal trends in the overall evolution of the seawater isotopic record through the Paleozoic. Maximum observed variation in the sulfur isotopes over each of the positive carbon isotope excursions decreases progressively through the Paleozoic, with a maximum of 24.5‰ for the SPICE event, 18.8‰ for the Silurian–Devonian boundary event, and 2.9‰ for the Early Mississippian

event. The decrease in sulfur isotope variability associated with each of the carbon isotope excursions of consistently large magnitude and direction suggests a change in the sensitivity of the marine sulfur reservoir to isotopic perturbation. The isotope record of the SPICE event reveals a Late Cambrian ocean reservoir that was sensitive to change, with large shifts in both carbon and sulfur isotope compositions of the ocean: 5‰ and 24‰, respectively. This parallel sensitivity may reflect the comparatively low concentrations of both sulfate and DIC in the Cambrian ocean—an observation for sulfur corroborated by fluid inclusion data from evaporites (Brennan et al., 2004) and models exploring the carbon isotope behavior of marine carbonates from the geologic record (Bartley and Kah, 2004). Relative to the SPICE, the Silurian–Devonian data show a more diminished response in the seawater sulfur isotope composition. Maximum sulfur variability of only 15‰ coincides with a carbon isotope event of equal magnitude to that of the SPICE. Finally, during the Early Mississippian carbon event, the $\delta^{34}\text{S}$ composition of the oceanic reservoir shows only 3‰ total variation in response to a perturbation in the carbon isotope record that is equivalent to those of the two earlier events.

We also should point out that our $\delta^{34}\text{S}_{\text{CAS}}$ results are consistent with the data reported by Kampschulte and Strauss (2004) for CAS and evaporites from the Paleozoic at widely different localities (see Fig. 1). More specifically, our data fall within the ranges represented in their data for each time interval, and the mean values generally match very closely. The idea of decreasing variability over the Paleozoic observed in our data is also manifested in the data of Kampschulte and Strauss (2004), corroborating that our short-term trends may be real and not simple products of diagenesis. For example, there is no straightforward argument for why diagenetic effects would have decreased over the Paleozoic. Also, large isotopic differences over small stratigraphic intervals are generally cited as evidence *against* wholesale diagenetic resetting. Again, this shorter-term isotopic behavior is superimposed on the long-recognized and modeled first-order Phanerozoic trend of Claypool et al. (1980), which is generally attributed to an overall shift in the masses of the oxidized and reduced reservoirs of carbon and sulfur.

Rates of sulfur isotope change can be calculated by dividing the observed isotopic shift by the estimated duration of each event. Durations for these events are well constrained through biostratigraphy and are considered to be on the order of 2–4 Myrs for the SPICE and 2 Myrs for the Silurian Devonian and Early Mississippian Events based on biostratigraphic constraints

(Saltzman et al., 1998, 2004; Buggisch and Mann, 2004). Due to uncertainties associated with the dating of the events we have used a broad range of ∂ts in our calculations, which are summarized in Table 5.

The resulting rates of isotopic variability ($\delta^{34}\text{S}/\partial t$) for the SPICE, Silurian–Devonian, and Early Mississippian events are summarized in Table 5. These rates are similar to those calculated by Kah et al. (2004) from $\delta^{34}\text{S}_{\text{CAS}}$ trends observed for the Mesoproterozoic and Neoproterozoic (0.8–10‰ Myr⁻¹) using conservative estimates for rates of sedimentation. Our maximum rates of isotopic change for the SPICE and Silurian–Devonian events actually exceed those of Kah et al. (2004). Collectively, these results reveal that the rapid variability seen in the Proterozoic sulfur isotope record extends into the Paleozoic. Younger shifts observed in the seawater $\delta^{34}\text{S}$ record are also not trivial. Nevertheless, Paleozoic variability and rates are appreciably greater than those recorded in the barite data of Paytan et al. (1998, 2004) from the Cretaceous, which show only 5‰ spreads over longer durations of 5 to 10 Myrs (1–0.5‰ Myr⁻¹).

Going a step further, the Kah et al. (2004) model and the calculated rates of isotopic change allow us to estimate the concentrations of sulfate in seawater based on the following equation:

$$M_o = [F_w \Delta S] / [\partial \delta_{\text{MAX}} / \partial t], \quad (2)$$

where M_o is the mass of sulfate in the ocean, F_w is the flux of sulfate to the ocean per year, ΔS is the fractionation between sulfate and sulfide, and $\partial \delta_{\text{MAX}} / \partial t$ is maximum rate of isotopic change. Further details of

the model are provided in Kah et al. (2004). Among the details discussed, Kah et al. applied a factor 10 correction to their Proterozoic $\delta^{34}\text{S}/\partial t$ estimates to account for assumed differences between the observed and maximum rates of isotopic variability. We have not applied this correction, instead assuming that our observed rates approach the maximum values. To justify this assumption, we note similarities between our observed rates and the maximum rates that we back-calculate from sulfate concentrations derived from coeval fluid inclusion data (Horita et al., 2002; Brennan et al., 2004; Lowenstein et al., 2005).

The calculated range of seawater sulfate concentrations for the SPICE, Silurian–Devonian boundary, and Early Mississippian events are summarized in Table 5 and Fig. 6. The estimated concentrations from the SPICE and Silurian–Devonian are similar to the range of values of 0.8 to 10.1 mM calculated by Kah et al. (2004) for the Proterozoic, which lends to the idea that low sulfate concentrations of the Proterozoic ocean persisted into the Paleozoic. Not surprisingly, our calculated concentrations from the SPICE and Silurian–Devonian boundary events are very similar to the values based on fluid inclusions marine halite reported by Horita et al. (2002), Brennan et al. (2004) for nearby time intervals (see Fig. 6), thus providing an independent check on our approach.

It should be pointed out that calculations for the Early Mississippian event for ∂ts greater than 1.25 Myr produce estimates of sulfate concentrations that are unreasonable (much greater than modern value of ~28 mM). This result is due to the behavior of our model at low $\partial \delta / \partial t$. However, concentrations calculated from lower ∂ts are in line with fluid inclusion data from marine halite for the Permian, the nearest time interval to our data (Horita et al., 2002; Lowenstein et al., 2005) and suggest durations for the event that are shorter than those implied tentatively.

The Paleozoic record is transitional between that of the Proterozoic ocean, with rapid sulfur isotope variability and low oceanic sulfate concentrations, and the more muted variability of the Mesozoic and Cenozoic. These patterns are all superimposed on the longer-term, first-order trend that occurs on time scales of 10⁷ to 10⁸ years. Proterozoic high-resolution CAS and gypsum records suggest rapid fluctuations in the seawater sulfur isotope composition. These fluctuations are attributed to limited availability of sulfate in the Precambrian ocean (Hurtgen et al., 2002; Kah et al., 2004; Gellatly and Lyons, 2005). Such deficiencies have been linked to comparatively low $p\text{O}_2$ in the Proterozoic atmosphere and correspondingly muted oxidative weathering of

Table 5
Model data

∂t (Myrs)	$\partial \delta / \partial t$ (‰/Myr)	SO_4^{2-} (mM)
<i>SPICE</i>		
0.8	30.6	2.5
1	24.5	3.1
2	12.3	6.2
4	6.1	12.4
<i>Silurian Devonian boundary</i>		
0.8	23.5	3.2
1	18.8	4.0
2	9.4	8.1
2.5	7.52	10.1
<i>Lower Mississippian</i>		
0.8	3.6	20.9
1	2.9	26.1
1.25	2.32	32.7
2	1.5	50.5 ^a

^a Data not included in Fig. 6.

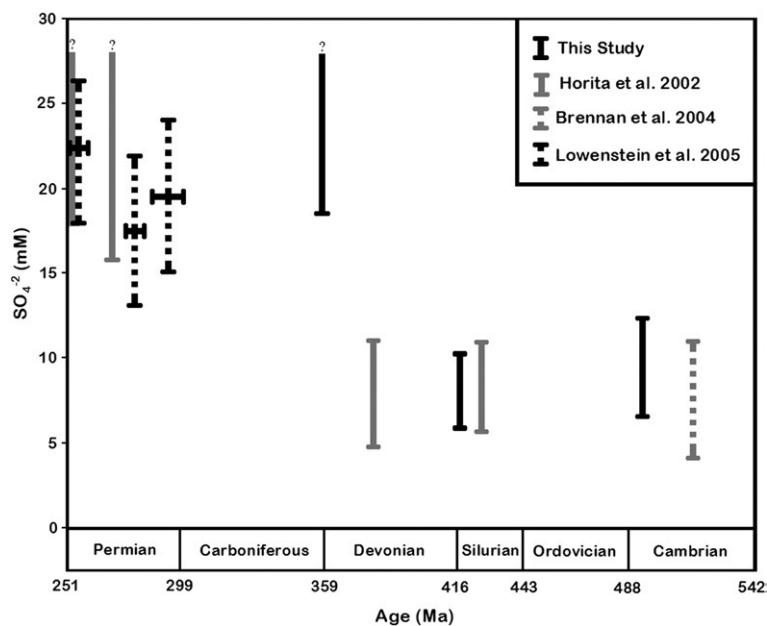


Fig. 6. Ranges of concentrations of marine sulfate during the Paleozoic. Our model data are in solid black compared to fluid inclusion data from marine halite in solid grey, dashed black, and dashed grey.

sulfides on the continents and thus flux of sulfate to the ocean (Kah et al., 2001, 2004; Gellatly and Lyons, 2005). Pervasive and persistent pyrite burial beneath a broadly oxygen-deficient Proterozoic deep ocean would also play a role (Canfield and Teske, 1996; Arnold et al., 2004; Hurtgen et al., 2005), and subduction of pyrite buried in deep ocean sediments may have further limited the accumulation of sulfate in the ocean (Canfield, 2004).

One possible explanation for the apparent change in sulfur isotope sensitivity from the Proterozoic and early Paleozoic to the late Paleozoic, assuming roughly similar perturbations to the flux relationships, is an increased mass of the marine sulfate reservoir. Concentration of sulfate in the global ocean is independently suggested to have increased through the Paleozoic based on fluid inclusion data from marine evaporites (Horita et al., 2002; Lowenstein et al., 2003, 2005; Brennan et al., 2004). Our modeling efforts (Fig. 6) also suggest an increase in the concentration of sulfate in seawater over the Paleozoic. This increase, which might have buffered the sulfur isotope composition despite in flux variations, can be attributed to at least two processes:

(1) *An end of deep ocean anoxia and pyrite burial.*

Deep oceanic anoxia may have persisted through the Proterozoic (Canfield and Teske, 1996; Arnold et al., 2004) and acted as a major sink for sulfur through the subduction of pyrite buried in deep ocean sediments (Canfield, 2004). The loss of this

output with eventual ventilation of the deep ocean would have facilitated the gradual buildup of sulfate in the oceanic reservoir over the Paleozoic.

- (2) *Increased pO_2 in the Earth's atmosphere over the Paleozoic.* Increased pO_2 in the Earth's atmosphere would have increased the rates of sulfide (principally pyrite) weathering on the continents and the flux of sulfate into the ocean. Concentrations of O_2 in the atmosphere likely increased through the Paleozoic, reaching a peak in the Carboniferous (Berner and Canfield, 1989; Berner and Petsch, 1998; Berner et al., 2000; Berner, 2001), reflecting the evolution, proliferation, and burial of land plants during the middle and late Paleozoic (Berner and Canfield, 1989). The marked decrease in the sulfur isotope variability and thus our calculated increase in sulfate concentration in Paleozoic seawater occurs between the Silurian–Devonian boundary and the Early Carboniferous, the interval marked by the initial proliferation of land plants.

A second, equally intriguing explanation for the apparent progressive decoupling of the carbon and sulfur isotope records is also linked to the rise of land plants. The burial of carbon on land would occur independent of significant pyrite burial because of the relatively low concentrations of sulfate in freshwater, while still driving positive carbon excursions in the ocean through

enhanced removal of ^{12}C from the global carbon cycle. Following land plant appearance in the middle Paleozoic, burial of their detritus became a large sink for organic carbon by the late Paleozoic (Bernier and Raiswell, 1983; Bernier and Canfield, 1989). Most likely all of the above processes had a hand in producing the high-resolution records sulfur records we observe. A combination of these controls is a possibility that we are exploring with numerical models.

6. Conclusions

The carbon and sulfur isotope records of the Paleozoic track an evolving oceanic reservoir and atmosphere. During the Phanerozoic, first-order sulfur and carbon isotope trends occurring on long time scales show a generally inverse relationship, reflecting the balance in the carbon and sulfur biogeochemical cycles that regulates oxygen content in the earth's atmosphere. Nevertheless, shorter-term variability is superimposed on this trend, capturing changes in source–sink relationships that are modulated by the size of the sulfur and carbon oceanic reservoirs and their evolving sensitivity to isotopic change. Early Paleozoic carbonates show a coupling between the carbon and sulfur isotope systems, with both sympathetic (SPICE event) and antithetic (Silurian–Devonian boundary) relationships between the two isotope systems. Carbonates from the Early Ordovician may capture the behavior of the ocean reservoir outside the influence of major perturbations in the carbon cycle. These $\delta^{34}\text{S}_{\text{CAS}}$ data suggest background invariance on at least 10^6 -year time scales—even early in the Paleozoic. Ongoing study of other sections stratigraphically removed from carbon excursions will test if the observations made from the Ordovician hold true more generally. Later records of the middle and late Paleozoic, although also preliminary, show a decoupling of the carbon and sulfur isotope records, which is manifested by a sharp decrease in $\delta^{34}\text{S}_{\text{CAS}}$ variability across large carbon excursions. A progressive decoupling of the short-term carbon and sulfur isotope systems over the duration of the Paleozoic may record an increasing oceanic sulfur reservoir against a backdrop of generally low DIC in the Paleozoic ocean. Also, a new locus of organic carbon burial, the terrestrial realm, permitted organic carbon sequestration in the absence of significant pyrite burial. Comparison of our sulfur data with those of other authors shows that the Paleozoic was a time of transition from a Proterozoic ocean with rapid isotopic variability to one with more gradual change in the Mesozoic and Cenozoic. Importantly, our data are among the first to document systematic (stratigraphic),

large magnitude and comparatively rapid sulfur isotope variability in the Paleozoic ocean—all facilitated by high-resolution sampling in a tight stratigraphic context. Remaining challenges include the distinction between local and global effects and sharpened mechanistic perspectives on carbon and sulfur cycling throughout the Paleozoic through numerical modeling of an expanded data set.

Acknowledgements

This work was funded by grants from the U.S. National Science Foundation: EAR-0418270 (TWL) and EAR-0418621 (MRS). We thank Steven Studley and Jon Fong of the Indiana Stable Isotope Lab for assistance with sulfur isotope analysis, Lora Wingate of the University of Michigan and Damon Basset of the University of Missouri Stable Isotope Lab for carbon isotope analyses, and Charles Gill and Greg Sitton for aid in fieldwork and sample collection. Many helpful discussions with Mike Formolo and Annie Gellatly contributed to the development and refinement of our laboratory techniques. We thank reviewers Scott Carpenter and Linda Kah for their helpful comments and Mike Pope for his editorial guidance and efforts in assembling this volume.

References

- Arnold, G.L., Anbar, A.D., Barling, J., Lyons, T.W., 2004. Molybdenum isotope evidence for widespread anoxia in mid-Proterozoic oceans. *Science* 304, 87–90.
- Ault, W.U., Kulp, J.L., 1959. Isotopic geochemistry of sulphur. *Geochimica et Cosmochimica Acta* 16, 201–235.
- Banner, J.L., Hanson, G.N., 1990. Calculation of simultaneous isotopic and trace element variations during water–rock interaction with applications to carbonate diagenesis. *Geochimica et Cosmochimica Acta* 54, 3123–3137.
- Bartley, J.K., Kah, L.C., 2004. Marine carbon reservoir, $\text{C}_{\text{org}}-\text{C}_{\text{carb}}$ coupling, and the evolution of the Proterozoic carbon cycle. *Geology* 32, 129–132.
- Berner, R.A., 1970. Sedimentary pyrite formation. *American Journal of Science* 268, 1–23.
- Berner, R.A., 1984. Sedimentary pyrite formation: an update. *Geochimica et Cosmochimica Acta* 48, 605–615.
- Berner, R.A., 1987. Models for carbon and sulfur cycles and atmospheric oxygen: application to Paleozoic geologic history. *American Journal of Science* 287, 177–190.
- Berner, R.A., 1989. Biogeochemical cycles of carbon and sulfur and their effect on atmospheric oxygen over Phanerozoic time. *Global and Planetary Change* 1, 97–122.
- Berner, R.A., 2001. Modeling atmospheric O_2 over Phanerozoic time. *Geochimica et Cosmochimica Acta* 65, 685–694.
- Berner, R.A., Canfield, D.E., 1989. A new model for atmospheric oxygen over Phanerozoic time. *American Journal of Science* 289, 333–361.

- Berner, R.A., Petsch, S.T., 1998. The sulfur cycle and atmospheric oxygen. *Science* 282, 1426–1427.
- Berner, R.A., Raiswell, R., 1983. Burial of organic carbon and pyrite sulfur in sediments over Phanerozoic time: a new theory. *Geochimica et Cosmochimica Acta* 47, 855–862.
- Berner, R.A., Petsch, S.T., Lake, J.A., Beerling, D.J., Popp, B.N., Lane, R.S., Laws, E.A., Westley, M.B., Cassar, N., Woodward, F.I., Quick, W.P., 2000. Isotope fractionation and atmospheric oxygen: implications for Phanerozoic O₂ evolution. *Science* 287, 1630–1633.
- Brand, U., 2004. Carbon, oxygen and strontium isotopes in Paleozoic carbonate components: an evaluation of original seawater-chemistry proxies. *Chemical Geology* 204, 23–44.
- Brennan, S.T., Lowenstein, T.K., Horita, J., 2004. Seawater chemistry and the advent of biocalcification. *Geology* 32, 473–476.
- Bruckschen, P., Veizer, J., 1997. Oxygen and carbon isotopic composition of Dinantian brachiopods: paleoenvironmental implications for the Lower Carboniferous of Western Europe. *Palaeogeography, Palaeoclimatology, Palaeoecology* 132, 243–264.
- Bruckschen, P., Oesmann, S., Veizer, J., 1999. Isotope stratigraphy of the European Carboniferous: proxy signals for ocean chemistry, climate and tectonics. *Chemical Geology* 161, 127–163.
- Brunner, B., Bernasconi, S.M., 2005. A revised isotope fractionation model for dissimilatory sulfate reduction in sulfate reducing bacteria. *Geochimica et Cosmochimica Acta* 69, 4759–4771.
- Buggisch, W., Mann, U., 2004. Carbon isotope stratigraphy of Lochkovian to Eifelian limestones from the Devonian of central and southern Europe. *International Journal of Earth Sciences* 93, 521–541.
- Buggisch, W., Keller, M., Lehnert, O., 2003. Carbon isotope record of Late Cambrian to Early Ordovician carbonates of the Argentine Precordillera. *Palaeogeography, Palaeoclimatology, Palaeoecology* 195, 357–373.
- Burdett, J.W., Arthur, M.A., Richardson, M., 1989. A Neogene seawater sulfur isotope age curve from calcareous pelagic microfossils. *Earth and Planetary Science Letters* 94, 189–198.
- Canfield, D.E., 2001. Isotope fractionation by natural populations of sulfate-reducing bacteria. *Geochimica et Cosmochimica Acta* 65, 1117–1124.
- Canfield, D.E., 2004. The evolution of the earth surface sulfur reservoir. *American Journal of Science* 304, 839–861.
- Canfield, D.E., Thamdrup, B., 1994. The production of ³⁴S-depleted sulfide during bacterial disproportionation of elemental sulfur. *Science* 266, 1973–1975.
- Canfield, D.E., Raiswell, R., Bottrell, S.H., 1992. The reactivity of sedimentary iron minerals toward sulfide. *American Journal of Science* 292, 659–683.
- Canfield, D.E., Teske, A., 1996. Late Proterozoic rise in atmospheric oxygen concentration inferred from phylogenetic and sulphur-isotope studies. *Nature* 382, 127–132.
- Carpenter, S.J., Lohmann, K.C., 1995. $\delta^{18}\text{O}$ and $\delta^{13}\text{C}$ values of modern brachiopod shells. *Geochimica et Cosmochimica Acta* 59, 3749–3764.
- Carpenter, S.J., Lohmann, K.C., 1997. Carbon isotope ratios of Phanerozoic marine cements: re-evaluating the global carbon and sulfur systems. *Geochimica et Cosmochimica Acta* 61, 4831–4846.
- Carpenter, S.J., Lohmann, K.C., 1999. Reply to the comment by S.T. Petsch on carbon isotope ratios of Phanerozoic marine cements: re-evaluating global carbon and sulfur systems. *Geochimica et Cosmochimica Acta* 63, 761–766.
- Cecile, M.P., Shakur, M.A., Krouse, H.R., 1983. The isotopic composition of western Canadian barites and the possible derivation of oceanic sulfate $\delta^{34}\text{S}$ and $\delta^{18}\text{O}$ age curves. *Canadian Journal of Earth Sciences* 20, 1528–1535.
- Claypool, G.E., Holser, W.T., Kaplan, I.R., Sakai, H., Zak, I., 1980. The age curves of sulfur and oxygen isotopes in marine sulfate and their mutual interpretation. *Chemical Geology* 28, 199–260.
- Cowan, C.A., Fox, D.L., Runkel, A.C., Saltzman, M.R., 2005. Terrestrial-marine carbon cycle coupling in ~500-m.y.-old phosphatic brachiopods. *Geology* 33, 661–664.
- Detmers, J., Bruchert, V., Habicht, K.S., Kuever, J., 2001. Diversity of sulfur isotope fractionation by sulfate-reducing prokaryotes. *Applied and Environmental Microbiology* 67, 888–894.
- Fike, D.A., Grotzinger, J.P., Pratt, L.M., Summons, R.E., 2006. Oxidation of the Ediacaran Ocean. *Nature* 444, 744–747.
- Frank, T.D., Lohmann, K.C., 1996. Diagenesis of fibrous magnesian calcite marine cement: implications for the interpretation of $\delta^{18}\text{O}$ and $\delta^{13}\text{C}$ values of ancient equivalents. *Geochimica et Cosmochimica Acta* 60, 2427–2436.
- Garrels, R.M., Lerman, A., 1981. Phanerozoic cycles of sedimentary carbon and sulfur. *PNAS* 78, 4652–4656.
- Gellatly, A.M., Lyons, T.W., 2005. Trace sulfate in mid-Proterozoic carbonates and sulfur isotope record of biospheric evolution. *Geochimica et Cosmochimica Acta* 69, 3813–3829.
- Glumac, B., Walker, K.R., 1998. A Late Cambrian positive carbon-isotope excursion in the Southern Appalachians; relation to biostratigraphy, sequence stratigraphy, environments of deposition, and diagenesis. *Journal of Sedimentary Research* 68, 1212–1222.
- Goldberg, T., Poulton, S.W., Strauss, H., 2005. Sulphur and oxygen isotope signatures of late Neoproterozoic to early Cambrian sulphate, Yangtze Platform, China: diagenetic constraints and seawater evolution. *Precambrian Research* 137, 223–241.
- Habicht, K.S., Canfield, D.E., 1996. Sulphur isotope fractionation in modern microbial mats and the evolution of the sulphur cycle. *Nature* 382, 342–343.
- Habicht, K.S., Canfield, D.E., 1997. Sulfur isotope fractionation during bacterial sulfate reduction in organic-rich sediments. *Geochimica et Cosmochimica Acta* 61, 5351–5361.
- Habicht, K.S., Canfield, D.E., 2001. Isotope fractionation by sulfate-reducing natural populations and the isotopic composition of sulfide in marine sediments. *Geology* 29, 555–558.
- Harrison, A.G., Thode, H.G., 1957. Mechanism of the bacterial reduction of sulphate from isotope fractionation studies. *Transactions of the Faraday Society* 54, 84–92.
- Hladikova, J., Hladil, J., Kibek, B., 1997. Carbon and oxygen isotope record across Pridoli to Givetian stage boundaries in the Barrandian basin (Czech Republic). *Palaeogeography, Palaeoclimatology, Palaeoecology* 132, 225–241.
- Holser, W.T., Kaplan, I.R., 1966. Isotope geochemistry of sedimentary sulfates. *Chemical Geology* 1, 93–135.
- Holser, W.T., Schidlowski, M., Mackenzie, F.T., Maynard, J.B., 1988. Geochemical cycles of carbon and sulfur. In: Gregor, C.B., Garrels, R.M., Mackenzie, F.T., Maynard, J.B. (Eds.), *Chemical Cycles in the Evolution of the Earth*. Wiley, New York, pp. 105–173.
- Horita, J., Zimmermann, H., Holland, H.D., 2002. Chemical evolution of seawater during the Phanerozoic: implications from the record of marine evaporites. *Geochimica et Cosmochimica Acta* 66, 3733–3756.
- Hurtgen, M.T., Arthur, M.A., Suits, N.S., Kaufman, A.J., 2002. The sulfur isotopic composition of Neoproterozoic seawater sulfate: implications for a snowball Earth? *Earth and Planetary Science Letters* 203, 413–429.
- Hurtgen, M.T., Arthur, M.A., Halverson, G.P., 2005. Neoproterozoic sulfur isotopes, the evolution of microbial sulfur species, and the burial efficiency of sulfide as sedimentary pyrite. *Geology* 33, 41–44.

- Kah, L.C., Lyons, T.W., Chesley, J.T., 2001. Geochemistry of a 1.2 Ga carbonate-evaporite succession, northern Baffin and Bylot Islands: implications for Mesoproterozoic marine evolution. *Precambrian Research* 111, 203–234.
- Kah, L.C., Lyons, T.W., Frank, T.D., 2004. Low marine sulphate and protracted oxygenation of the Proterozoic biosphere. *Nature* 431, 834–838.
- Kampschulte, A., Strauss, H., 2004. The sulfur isotopic evolution of Phanerozoic seawater based on the analysis of structurally substituted sulfate in carbonates. *Chemical Geology* 204, 255–286.
- Kampschulte, A., Bruckschen, P., Strauss, H., 2001. The sulphur isotopic composition of trace sulphates in Carboniferous brachiopods: implications for coeval seawater, correlation with other geochemical cycles and isotope stratigraphy. *Chemical Geology* 175, 149–173.
- Kaufman, A.J., Hayes, J.M., Knoll, A.H., Germs, G.J.B., 1991. Isotopic compositions of carbonates and organic carbon from upper Proterozoic successions in Namibia: stratigraphic variation and the effects of diagenesis and metamorphism. *Precambrian Research* 49, 301–327.
- Kemp, A.L.W., Thode, H.G., 1968. The mechanism of the bacterial reduction of sulphate and of sulphite from isotope fractionation studies. *Geochimica et Cosmochimica Acta* 32, 71–91.
- Kump, L.R., 1989. Alternate modeling approaches to the geochemical cycles of carbon, sulfur, and strontium isotopes. *American Journal of Science* 289, 390–410.
- Kump, L.R., Garrels, R.M., 1986. Modeling atmospheric O₂ in the global sedimentary redox cycle. *American Journal of Science* 286, 337–360.
- Kump, L.R., Arthur, M.A., Patzkowsky, M.E., Gibbs, M.T., Pinkus, D.S., Sheehan, P.M., 1999. A weathering hypothesis for glaciation at high atmospheric pCO₂ during the Late Ordovician. *Palaeogeography, Palaeoclimatology, Palaeoecology* 152, 173–187.
- Lowenstein, T.K., Hardie, L.A., Timofeeff, M.N., Demicco, R.V., 2003. Secular variation in seawater chemistry and the origin of calcium chloride basinal brines. *Geology* 31, 857–860.
- Lowenstein, T.K., Timofeeff, M.N., Kovalevych, V.M., Horita, J., 2005. The major-ion composition of Permian seawater. *Geochimica et Cosmochimica Acta* 69, 1701–1719.
- Lyons, T.W., Gill, B.C., Shim, M.J., Frank, T.D., Hurtgen, M.T., Saltzman, M.R., Gellatly, A.M., Kah, L.C., 2004a. Carbonate-associated sulfate as a paleoceanographic proxy: an update. *Geochimica et Cosmochimica Acta* 68, 337.
- Lyons, T.W., Walter, L.M., Gellatly, A.M., Martini, A.M., Blake, R.E., 2004b. Sites of anomalous organic remineralization in the carbonate sediments of South Florida, USA: the sulfur cycle and carbonate-associated sulfate. *Geological Society of America Special Paper* 379, 161–176.
- Mii, H.s., Grossman, E.L., Yancey, T.E., 1999. Carboniferous isotope stratigraphies of North America: implications for Carboniferous paleoceanography and Mississippian glaciation. *Geological Society of America Bulletin* 111, 960–973.
- Newton, R.J., Pevitt, E.L., Wignall, P.B., Bottrell, S.H., 2004. Large shifts in the isotopic composition of seawater sulphate across the Permo-Triassic boundary in northern Italy. *Earth and Planetary Science Letters* 218, 331–345.
- Ohkouchi, N., Kawamura, K., Kajiwar, Y., Wada, E., Okada, M., Kanamatsu, T., Taira, A., 1999. Sulfur isotope records around Livello Bonarelli (northern Apennines, Italy) black shale at the Cenomanian–Turonian boundary. *Geology* 27, 535–538.
- Overstreet, R.B., Ohoh-Ikenobe, F.E., Gregg, J.M., 2003. Sequence stratigraphy and depositional facies of Lower Ordovician cyclic carbonate rocks, southern Missouri, U.S.A. *Journal of Sedimentary Research* 73, 421–433.
- Parkinson, D., Curry, G.B., Cusack, M., Fallick, A.E., 2005. Shell structure, patterns and trends of oxygen and carbon stable isotopes in modern brachiopod shells. *Chemical Geology* 219, 193–235.
- Paytan, A., Kastner, M., Campbell, D., Thiemens, M.H., 1998. Sulfur isotopic composition of Cenozoic seawater sulfate. *Science* 282, 1459–1462.
- Paytan, A., Kastner, M., Campbell, D., Thiemens, M.H., 2004. Seawater sulfur isotope fluctuations in the Cretaceous. *Science* 304, 1663–1665.
- Petsch, S.T., Berner, R.A., 1998. Coupling the geochemical cycles of C, P, Fe, and S: the effect on atmospheric O₂ and the isotopic records of carbon and sulfur. *American Journal of Science* 298, 246–262.
- Pingitore, J., Nicholas, E., Meitzner, G., Love, K.M., 1995. Identification of sulfate in natural carbonates by X-ray absorption spectroscopy. *Geochimica et Cosmochimica Acta* 59, 2477–2483.
- Popp, B.N., Anderson, T.F., Sandberg, P.A., 1986. Brachiopods as indicators of original isotopic compositions in some Paleozoic limestones. *Geological Society of America Bulletin* 97, 1262–1269.
- Qing, H., Veizer, J., 1994. Oxygen and carbon isotopic composition of Ordovician brachiopods: implications for coeval seawater. *Geochimica et Cosmochimica Acta* 58, 4429–4442.
- Raab, M., Spiro, B., 1991. Sulfur isotopic variations during seawater evaporation with fractional crystallization. *Chemical Geology. Isotope Geoscience Section* 86, 323–333.
- Riccardi, A.L., Arthur, M.A., Kump, L.R., 2006. Sulfur isotopic evidence for chemocline upward excursions during the Permian mass extinction. *Geochimica et Cosmochimica Acta* 70, 5740–5752.
- Saltzman, M.R., 2002a. Carbon and oxygen isotope stratigraphy of the Lower Mississippian (Kinderhookian–lower Osagean), western United States: implications for seawater chemistry and glaciation. *Geological Society of America Bulletin* 114, 96–108.
- Saltzman, M.R., 2002b. Carbon isotope ($\delta^{13}\text{C}$) stratigraphy across the Silurian–Devonian transition in North America: evidence for a perturbation of the global carbon cycle. *Palaeogeography, Palaeoclimatology, Palaeoecology* 187, 83–100.
- Saltzman, M.R., Runnegar, B., Lohmann, K.C., 1998. Carbon isotope stratigraphy of Upper Cambrian (Steptoean Stage) sequences of the eastern Great Basin: record of a global oceanographic event. *Geological Society of America Bulletin* 110, 285–297.
- Saltzman, M.R., Ripperdan, R.L., Brasier, M.D., Lohmann, K.C., Robison, R.A., Chang, W.T., Peng, S., Ergaliev, E.K., Runnegar, B., 2000. A global carbon isotope excursion (SPICE) during the Late Cambrian: relation to trilobite extinctions, organic-matter burial and sea level. *Palaeogeography, Palaeoclimatology, Palaeoecology* 162, 211–223.
- Saltzman, M.R., Groessens, E., Zhuravlev, A.V., 2004. Carbon cycle models based on extreme changes in $\delta^{13}\text{C}$: an example from the lower Mississippian. *Palaeogeography, Palaeoclimatology, Palaeoecology* 213, 359–377.
- Shields, G., Kimura, H., Yang, J., Gammon, P., 2004. Sulphur isotopic evolution of Neoproterozoic–Cambrian seawater: new francolite-bound sulphate $\delta^{34}\text{S}$ data and a critical appraisal of the existing record. *Chemical Geology* 204, 163–182.
- Silberling, N.J., Nichols, K.M., Trexler, J.H.J., Jewell, P.W., Crosbie, R.A., 1997. Overview of Mississippian depositional and paleotectonic history of the Antler Foreland, eastern Nevada and western Utah. *Geology Studies* 42, 161–196.
- Staudt, W.J., Schoonen, M.A.A., 1995. Sulfate incorporation into sedimentary carbonates. In: Vairavamurthy, M.A., Schoonen, M.A.A.

- (Eds.), *Geochemical Transformations of Sedimentary Sulfur*. American Chemical Society, Washington, D.C., pp. 332–345.
- Strauss, H., 1997. The isotopic composition of sedimentary sulfur through time. *Palaeogeography, Palaeoclimatology, Palaeoecology* 132, 97–118.
- Strauss, H., 1999. Geological evolution from isotope proxy signals—sulfur. *Chemical Geology* 161, 89–101.
- Takano, B., 1985. Geochemical implications of sulfate in sedimentary carbonates. *Chemical Geology* 49, 393–403.
- Thode, H.G., Monster, J., Dunford, H.B., 1961. Sulphur isotope geochemistry. *Geochimica et Cosmochimica Acta* 25, 159–174.
- Ueda, A., Campbell, F.A., Krouse, H.R., Spencer, R.J., 1987. $^{34}\text{S}/^{32}\text{S}$ Variations in trace sulphide and sulphate in carbonate rocks of a Devonian reef, Alberta, Canada, and the Precambrian Siyeh formation, Montana, U.S.A. *Chemical Geology. Isotope Geoscience Section* 65, 383–390.
- Ueda, A., Cameron, E.M., Roy Krouse, H., 1991. ^{34}S -enriched sulphate in the Belcher Group, N.W.T., Canada: evidence for dissimilatory sulphate reduction in the early Proterozoic ocean. *Precambrian Research* 49, 229–233.
- Veizer, J., Holser, W.T., Wilgus, C.K., 1980. Correlation of $^{13}\text{C}/^{12}\text{C}$ and $^{34}\text{S}/^{32}\text{S}$ secular variations. *Geochimica et Cosmochimica Acta* 44, 579–587.
- Veizer, J., Fritz, P., Jones, B., 1986. Geochemistry of brachiopods: oxygen and carbon isotopic records of Paleozoic oceans. *Geochimica et Cosmochimica Acta* 50, 1679–1696.
- Veizer, J., Ala, D., Azmy, K., Bruckschen, P., Buhl, D., Bruhn, F., Carden, G.A.F., Diener, A., Ebner, S., Godderis, Y., 1999. $^{87}\text{Sr}/^{86}\text{Sr}$, $\delta^{13}\text{C}$ and $\delta^{18}\text{O}$ evolution of Phanerozoic seawater. *Chemical Geology* 161, 59–88.